Published in final edited form as:
J Struct Biol. 2012 February ; 177(2): 224–232. doi:10.1016/j.jsb.2011.09.003.

Soft X-ray microscopy analysis of cell volume and hemoglobin content in erythrocytes infected with asexual and sexual stages of *Plasmodium falciparum*

Eric Hanssen[a,*], **Christian Knoechel**[b], **Megan Dearnley**[c,d], **Matthew W.A. Dixon**[c,d], **Mark Le Gros**[b], **Carolyn Larabell**[b,e], and **Leann Tilley**[c,d]

[a]Electron Microscopy Unit, Bio21 Molecular Science and Biotechnology Institute, and ARC Centre of Excellence for Coherent X-ray Science, The University of Melbourne, Melbourne, VIC 3010, Australia

[b]Physical Bioscience Division, Lawrence Berkeley National Laboratory, CA, USA

[c]Department of Biochemistry, La Trobe University, and ARC Centre of Excellence for Coherent X-ray Science, Bundoora, VIC 3086, Australia

[d]Department of Biochemistry and Molecular Biology, Bio21 Molecular Science and Biotechnology Institute, The University of Melbourne, Melbourne, VIC 3010, Australia

[e]Department of Anatomy, University of California, San Francisco, CA, USA

Abstract

Plasmodium falciparum, the most virulent agent of human malaria, undergoes both asexual cycling and sexual differentiation inside erythrocytes. As the intraerythrocytic parasite develops it increases in size and alters the permeability of the host cell plasma membrane. An intriguing question is: how is the integrity of the host erythrocyte maintained during the intraerythrocytic cycle? We have used water window cryo X-ray tomography to determine cell morphology and hemoglobin content at different stages of asexual and sexual differentiation. The cryo stabilization preserves native structure permitting accurate analyses of parasite and host cell volumes. Absorption of soft X-rays by protein adheres to Beer–Lambert's law permitting quantitation of the concentration of hemoglobin in the host cell compartment. During asexual development the volume of the parasite reaches about 50% of the uninfected erythrocyte volume but the infected erythrocyte volume remains relatively constant. The total hemoglobin content gradually decreases during the 48 h cycle but its concentration remains constant until early trophozoite stage, decreases by 25%, then remains constant again until just prior to rupture. During early sexual development the gametocyte has a similar morphology to a trophozoite but then undergoes a dramatic shape change. Our cryo X-ray tomography analysis reveals that about 70% of the host cell hemoglobin is taken up and digested during gametocyte development and the parasite eventually occupies about 50% of the uninfected erythrocyte volume. The total volume of the infected erythrocyte remains constant, apart from some reversible shrinkage at stage IV, while the concentration of hemoglobin decreases to about 70% of that in an uninfected erythrocyte.

[*]Corresponding author. Address: Electron Microscopy Unit, Bio21 Institute, The University of Melbourne, 30 Flemington Road, Melbourne, VIC 3010, Australia. Fax: +61 383442515. ehanssen@unimelb.edu.au (E. Hanssen)..

Appendix A. Supplementary data

Supplementary data associated with this article can be found, in the online version, at doi:10.1016/j.jsb.2011.09.003.

Keywords

Plasmodium; Tomography; X-ray; Hemoglobin; Gametocyte

1. Introduction

Malaria affects more than 240 million people annually resulting in about 781,000 deaths (WHO, 2010). *Plasmodium falciparum* causes the majority of the deaths and produces the most severe clinical manifestations, with symptoms ranging from uncomplicated fevers to life-threatening cerebral and placental malaria (Miller et al., 2002; Rowe et al., 2009). The malaria parasite spends part of its lifecycle inside the red blood cells (RBCs) of its human host. Over a period of 44–48 h it develops through the ring and trophozoite stages, then divides to form an average of ~20 daughter cells in the schizont stage (Tilley et al., 2011).

The intraerythrocytic parasite grows in size from an initial diameter of about 1 μm to a schizont with a diameter of about 6 μm. A question that has intrigued researchers is: how does the parasite prevent swelling and premature lysis of the host RBC? For example, it has been suggested that a 1.7-fold increase in RBC volume would result in host cell lysis (Lew et al., 2003). Volume control becomes a particular challenge in the early trophozoite stage, when there is a marked increase in the permeability of the RBC membrane to low molecular weight solutes. This is due to the induction of novel permeability pathways (NPP) which are thought to play important roles in the delivery of nutrients and the efflux of waste products (Lew et al., 2003; Nguitragool et al., 2011). One consequence of the establishment of the NPPs is the dissipation of the Na^+ and K^+ gradients across the RBC membrane. This facilitates phosphate uptake (Saliba et al., 2006), but compromises the normal mechanisms for volume control (Martin and Kirk, 2007).

One mechanism that the parasite uses to control the volume of the host cell is ingestion and degradation of hemoglobin. The intraerythrocytic parasite takes up small packets of the host cell cytoplasm using endocytic structures called cytostomes. It transfers the hemoglobin to an acidic digestive vacuole (Abu Bakar et al., 2010), where it is degraded by proteases (Goldberg, 2005; Loria et al., 1999). About 15% of the liberated amino acids are used for protein synthesis and the rest are exported to the extracellular medium (Krugliak et al., 2002). The hematin that is produced as a by-product of hemoglobin digestion is sequestered into a crystalline form known as hemozoin and is retained within the digestive vacuole (Pagola et al., 2000).

It has been postulated that hemoglobin digestion and efflux of the amino acids is used to prevent excessive swelling of the host cell (Lew et al., 2003). Nonetheless, early modelling predicted that the volume of the infected RBC would approach the point of hemolysis and that hemoglobin digestion must exceed parasite growth in order to avoid lysis (Lew et al., 2004; Staines et al., 2001). By contrast experimental data suggests that any changes in the volume of the infected RBCs are moderate, with a moderate decrease (Zanner et al., 1990), a moderate increase (Esposito et al., 2010), and no change (Saliba et al., 1998) reported by different authors. Available estimates of the hemoglobin concentration in the host cell cytoplasm indicate that it decreases, but these measurements have mostly relied on indirect approaches.

After a period of asexual cycling, in response to poorly defined environmental cues, a small proportion of parasites commit to forming gametocytes (Alano, 2007). This involves a remarkable series of morphological changes as the parasite prepares for sexual reproduction in the mosquito. Early gametocytes are morphologically indistinguishable from early

asexual parasites but later stage gametocytes elongate to adopt a characteristic crescent or falciform shape unique to *P. falciparum* (Alano, 2007; Dixon et al., 2008). Hemoglobin digestion occurs during gametocyte development with the resultant production of hemozoin (Lang-Unnasch and Murphy, 1998; Sinden, 1982). Until now, however, there has been no analysis of changes in the concentration of hemoglobin in the host cell compartment during gametocyte development, nor a detailed analysis of the volumes of different compartments. It is thus of interest to determine if similar mechanisms for volume control are employed in the gametocyte stage.

Cryo X-ray tomography has recently been introduced as a high resolution, low artifact technique that can be performed on whole hydrated cells (Larabell and Le Gros, 2004; Le Gros et al., 2005; Parkinson et al., 2008; Uchida et al., 2009). The differential absorption of soft X-rays by organic matter and water provides natural contrast and avoids the need for exogenous stains or chromophores. We have recently used cryo X-ray tomography to survey the cellular features of *P. falciparum* (Hanssen et al., 2011). In this work we have made use of the fact that X-ray absorbance is directly related to the concentration of absorbing species to undertake a comparative analysis of the concentration of hemoglobin in the host cell at different stages of asexual and sexual development.

2. Materials and methods

2.1. Parasites

P. falciparum was cultured *in vitro* in RPMI medium supplemented with 4% human serum plus 0.25% AlbuMAX (GIBCO, Invitrogen) as described previously (Jackson et al., 2007). RBCs and pooled sera were obtained from the Red Cross Blood Service (Melbourne, Australia) or from volunteers (ALS, Berkeley, USA). Mature stage-infected RBCs were harvested by flotation on a Percoll/sorbitol gradient (Aley et al., 1986) or using a magnetized column (Trang et al., 2004). Similar morphology of infected RBCs was observed using these different enrichment methods.

Gametocytes were prepared using a modification of a published protocol (Fivelman et al., 2007). A culture of mainly ring stage parasites (6–8% parasitemia) was treated with 5% sorbitol (Lambros and Vanderberg, 1979), then separated using a Percoll density gradient (Knight and Sinden, 1982) to enrich the ring stage and remove any gametocytes. The parasites were cultured till they reached 8–10% trophozoites, then sub-divided to 2% trophozoites (5% hematocrit). The culture was maintained for 10 days in the presence of 62.5 mM *N*-acetyl glucosamine to inhibit merozoite invasion and thus asexual replication (Hadley et al., 1986; Ponnudurai et al., 1986). Giemsa-stained slides and immunofluorescence microscopy using the gametocyte-specific marker, anti-Pfs16 (Alano et al., 1991; Dixon et al., 2009), were used to monitor stage progression. The medium was changed daily but no fresh RBCs were added. Gametocytes were enriched at the desired stages of development by magnetic separation.

2.2. Protein solutions

A bovine serum albumin (BSA) stock solution (5 mM) was prepared from powdered BSA (Sigma) in PBS. A hemoglobin solution was prepared using a modification of a published protocol (Rabiner et al., 1967). Briefly an aliquot of packed RBCs was mixed for 10 min with an equal volume of distilled water, then centrifuged at 17,000g for 10 min. The supernatant was filtered through a 0.22 μm filter and the concentration determined spectrophotometrically (Snell and Marini, 1988).

2.3. X-ray tomography

Aliquots of live mixed asexual stage cultures (high parasitemia, mostly early stages) or harvested late stage-infected RBCs, or enriched gametocytes, were loaded into 4-6 μm capillaries using an electrophoresis tip. Capillaries were pre-treated with poly-L-lysine (0.01%; Sigma) and dipped in 100 nm colloidal gold (Sigma) under a constant air flow (Eppendorf Femtojet). The capillaries were rapidly frozen in liquid nitrogen and mounted in a cryogenic gas stream (liquid nitrogen cooled helium gas) (Le Gros et al., 2005). Projection images were collected using a transmission soft X-ray microscope (XM-2; beamline 2.1.2 at the Advanced Light Source, Lawrence Berkeley National Laboratory, Berkeley, CA). The microscope is equipped with a Fresnel zone plate condenser and objective (with 60 and 50 nm outer zone widths, respectively). Data were collected as described previously (Hanssen et al., 2011). The IMOD package (Kremer et al., 1996; Mastronarde, 1997) was used to align the individual images. Tomographic reconstructions were calculated using iterative methods (Erdogan and Fessler, 1999; Stayman and Fessler, 2000). Segmentation models were generated with 3dmod (http://bio3d.colorado.edu/) and Blender (www.blender.org). The parasite and host cells were segmented manually using 3dmod and volumes and surface areas estimated using the IMODinfo routine.

2.4. X-ray absorption measurements

Volumes were created in different parts of the host cell cytoplasm or in different regions of the BSA or hemoglobin samples and average pixel values were measured using the sum density routine included in the IMOD package. For calibration of the X-ray absorption, BSA and hemoglobin were serially diluted in water.

2.5. Electron microscopy

Infected RBCs were fixed in 2.5% glutaraldehyde in 0.1 M sodium cacodylate, post fixed with 1% osmium tetroxide and 'en-bloc' stained with 1% uranyl acetate. Cells were serially dehydrated and embedded in LRWhite resin. Sections (70 nm) were cut and stained with uranyl acetate and lead citrate and observed at 200 kV on a Tecnai G^2 F30 (Bio21 Institute, Melbourne).

3. Results

3.1. Relationship between the X-ray absorption coefficient and the protein concentration

In order to test the linearity of soft X-ray absorption as a function of protein concentration in the XM-2 transmission X-ray microscope we loaded soluble protein samples into glass capillaries for imaging under cryo-conditions. Cross sections of capillaries containing different dilutions of BSA are presented in Fig. 1A and the absorption coefficients in Fig. 1B. We also extracted cytosol from RBCs and measured the absorption coefficient as a function of the estimated hemoglobin concentration (Fig. 1C). The slope was used to calculate the hemoglobin concentration in uninfected and infected RBCs.

3.2. Morphology of parasitized RBCs

We examined the X-ray absorption profiles of *P. falciparum* at different stages of development. Infected RBCs were harvested, loaded into capillaries, rapidly frozen and mounted in the microscope chamber. A series of projection images collected during rotation through 180° were aligned to generate a tomogram. Individual virtual sections through the *z*-plane of the capillaries in regions containing uninfected RBCs and ring, early and late trophozoite and schizont stage-infected RBC are shown in Fig. 2. The ring stage parasite (Fig. 2A and E) is cup-shaped with a large invagination (black arrowhead) of the host cytoplasm as illustrated in the rendered model (bottom panel). The early trophozoite

maintains an invagination feature (Fig. 2B and F, black arrowheads) but by mid-trophozoite stage the parasite expands to a more spherical shape and X-ray dense features are evident within the parasite; these are aggregates of hemozoin crystals (Fig. 2B–D, white arrows; Fig. 2F–G, rendered in red). One or two X-ray dense spherical structures are observed close to the crystal-loaded digestive vacuole (Fig. 2C, white arrowhead). These likely represent neutral lipid bodies (Jackson et al., 2004), though further work is needed to confirm this. Individual merozoites (m) are evident in a schizont-infected RBC (Fig. 2D and H), each with a pair of X-ray dense apical organelles (Fig. 2H, rendered in green).

In electron tomography of plastic-embedded samples, the harsh fixation and dehydration processes required for sample preparation, as well as the shrinkage of the sample that occurs during imaging, confound any morphometric measurements. By contrast samples imaged by cryo X-ray microscopy do not show any obvious cellular damage during cryo stabilization and there is no evidence for gross shrinkage or photon damage during the imaging process. The tomograms can therefore be used to measure volume and surface area (Fig. 3). The following parasite volumes were determined: mid ring stage (1.7 ± 0.5 fL (n = 5)), young trophozoite stage (1 nucleus; 9.0 ± 1.5 fL (n = 5)), mid trophozoite (2 nuclei; 18.0 ± 3.5 fL (n = 6)), late trophozoite (4 nuclei; 33.0 ± 6.0 fL (n = 6)), early schizont (8 nuclei; 41.0 ± 4.0 fL (n = 6)), mid schizont (16 nuclei; 35.5 ± 1.5 fL (n = 5)) and late segmented schizont (37.0 ± 1.0 fL (n = 4)).

The data show that the parasite volume expands during the ring and trophozoite stages and then stabilizes once it reaches the 8 nuclei stage (Fig. 3A). By contrast the infected RBC volume stays relatively constant (Fig. 3B) with respective values of 86.0 ± 16.0 fL (uninfected RBCs, n = 5), 84.5 ± 16.0 fL (ring), 78.5 ± 13.5 fL (young trophozoite), 87.5 ± 19.5 fL (mid trophozoite), 79.0 ± 14.5 fL (late trophozoite), 70.5 ± 10.0 fL (early schizont), 68.0 ± 9.0 fL (late schizont) and 90.0 ± 27.0 fL (segmented schizont).

3.3. Hemoglobin concentration in asexual stage-infected RBCs

The absorption coefficients of several small volumes within the host cell cytoplasm of RBCs infected with different parasite stages were determined and averaged. The estimated concentration of the hemoglobin tetramer in uninfected RBCs is 4.9 ± 0.5 mM (Fig. 3C), which is within the normal clinical range (4.9–5.5 mM (MedlinePlus)). The hemoglobin concentration remains stable until the first nuclear division, even though the parasite increases substantially in size. The estimated concentrations are 4.9 ± 0.5 mM (ring) and 5.4 ± 0.6 mM (early trophozoite). After this point the concentration decreases sharply and remains lower: 3.5 ± 0.3 mM (mid trophozoite); 3.9 ± 0.5 mM (late trophozoite); 4.1 ± 0.6 mM (early schizont); 3.8 ± 0.2 mM (mid schizont). There is a further decrease to 2.7 ± 0.2 mM in the segmented schizont.

While the hemoglobin concentration exhibits two stable phases separated by a sharp transition, the total amount of hemoglobin per cell decreases slowly during the ring stage and then more sharply during the trophozoite stages (1–4 nuclei) (Fig. 3D). The estimated values are 28.5 ± 4.5 pg (uninfected RBCs), 27.5 ± 4.0 pg (ring), 25.0 ± 1.5 pg (early trophozoite), 16.0 ± 2.5 pg (mid trophozoite), 12.5 ± 4.0 pg (late trophozoite), 8.5 ± 3.0 pg (early schizont), 8.5 ± 2.0 pg (mid schizont) and 9.5 ± 4.5 pg (segmented schizont). Digestion appears to be completed by the 8 nuclei schizont stage with no further decrease in the total quantity of hemoglobin in the cell.

3.4. Gametocyte morphology

While asexual stage parasites have been extensively studied, the morphology and volume control of gametocytes is much less investigated. We generated gametocytes using

established protocols and followed them for a period of 7–10 days. We were able to obtain multiple datasets for gametocytes at stages II–V (Fig. 4). Stage II is the first stage that can be morphologically distinguished from the asexual trophozoite stage. At this stage the parasite remains roughly spherical with a similar-shaped nucleus (Fig. 4A and B). The shape is similar to that of an asexual trophozoite, however, it has only one nucleus while an asexual parasite of the same size (30.5 ± 9.5 fL, see Fig. 5A) would have four nuclei. Moreover in some discrete regions around the parasite cryo X-ray microscopy reveals a thickening of the parasite pellicle at this stage (Fig. 4L), which is not present in a trophozoite-infected RBC (Fig. 4K). This likely corresponds to the tri-laminar membrane structure and underlying microtubules known as the sub-pellicular membrane complex (Sinden and Smalley, 1979). The presence of multiple crystals of hemozoin provides evidence that substantive hemoglobin digestion has already taken place.

By stage III of gametocyte development (Fig. 4C and D) one edge of the parasite has straightened and extended as the parasite starts to adopt a “hat-shape” morphology. Additional features are observed in the parasite cytoplasm. As well as the X-ray dense hemozoin crystals, we observed X-ray lucent vacuoles (v), and structures of medium X-ray absorption per unit volume (white arrowhead), that likely represent the mitochondrion, which is readily identified by electron microscopy (Fig. 4M). The X-ray-dense spherical structures (likely neutral lipid bodies) that are observed in a sexual stages do not appear to form in the sexual stage. By this stage the host cell is reduced to a thin layer around the parasite and a flattened extension, referred to as the Laveran’s bib (asterisk).

Stage IV gametocytes have undergone further elongation, with straightening along the other edge of the cell and evidence of the sub-pellicular membrane complex around the entire perimeter of the cell. There is a particular thickening of the sub-pellicular membrane complex density at the extremities of the cell (Fig. 4E and F). Again low density vacuoles, the mitochondrion and hemozoin crystals are readily observed. At this stage osmophillic bodies (Sinden et al., 1978) begin to be distinguishable.

In stage V gametocytes the ends of the parasite become more rounded, the osmophillic bodies more pronounced, and the low density vacuoles enlarged (Fig. 4G–J; Supplementary Movie 1). In female gametocytes, including the cell depicted in Fig. 4G and H, the hemozoin crystals coalesce in one or two main regions near the centre of the cell. In the less numerous male gametocytes the hemozoin crystals are more dispersed (Fig. 4I and J).

The volume of the parasite remains roughly constant from stage III to stage IV (Fig. 5A) although there appears to be a transient decrease in volume at stage IV. Similarly the volume of the infected RBC remains similar to that of an uninfected RBC (Fig. 5B), again apart from a transient decrease in stage IV. The surface area of the sexual stage-infected RBC is constant throughout (data not shown). The volumes for stage II, III, IV and V parasites are: 30.5 ± 9.5 fL (n = 6), 37.0 ± 6.0 fL (n = 5), 28.5 ± 2.5 fL (n = 4), 41.0 ± 12.0 fL (n = 7). The volumes of the infected RBCs are 86.0 ± 16.0 fL (uninfected RBCs, n = 5), 78.0 ± 10.0 fL (stage II), 74.5 ± 9.0 fL (stage III), 54.0 ± 11.0 fL (stage IV) and 73.5 ± 20.5 fL (stage V).

Gametocytes undergo dramatic shape changes during their maturation with a major elongation in one axis from stage II to IV and a relaxation in stage V, while the diameter decreases from stage II to IV, then increases in stage V (Fig. 5C). The lengths and diameters are respectively 4.3 ± 0.5/3.6 ± 0.6 μm, 7.4 ± 1.7/3.3 ± 0.3 μm, 11.0 ± 1.2/2.6 ± 0.1 μm, 8.7 ± 0.9/3.0 ± 0.4 μm.

3.5. Hemoglobin concentration in the host RBC during gametocytogenesis

The concentration of hemoglobin in the host RBC decreases gradually during differentiation from stage II to stage V (Fig. 6A) with respective values of 5.0 ± 0.5 mM (uninfected RBCs, $n = 8$), 4.3 ± 0.6 mM (stage II), 3.9 ± 0.5 mM (stage III), 4.0 ± 0.7 (stage IV) and 3.5 ± 0.8 mM (stage V). By contrast the total amount of hemoglobin (Fig. 6B) in the stage II gametocyte (14.0 ± 2.0 pg) is much less than that for uninfected RBCs (28.5 ± 4.5 pg) and similar to that of a mid to late asexual trophozoite (Fig. 3C). The quantity decreases slightly in stage III (9.5 ± 2.5 pg) and stage IV (8.0 ± 4.0), then remains stable in stage V (7.5 ± 2.5 pg) suggesting that digestion is completed by stage IV. This is supported by the fact that the volume of hemozoin crystals remains roughly constant in the later stages of development (Fig. 6C).

4. Discussion

X-ray microscopy can provide details of the internal structure of thick (~10 μm), hydrated, unstained sections or whole cells (Gu et al., 2007; Le Gros et al., 2005; Uchida et al., 2009). The cryo-capability that has been implemented in the XM-2 microscope helps limits X-ray damage during imaging and we observed no evidence for gross shrinkage or disruption of the sample during data collection. The tomographic capability of XM-2 and its improved optics allow a major enhancement of image quality with correspondingly higher information content.

The “water window” is the region of the X-ray spectrum between the K shell absorption edges of carbon (4.4 nm) and oxygen (2.3 nm). X-rays in this region are absorbed approximately ten times more strongly by carbon- and nitrogen-containing material than by water. The absorption adheres to the Beer-Lambert’s law and is therefore linear with thickness and concentration. Unhydrated carbon-rich materials (e.g. lipids) show a particularly high absorption. Thus the absorption profile can provide quantitative information about the concentration and likely composition of different cellular compartments.

In this work we have performed a cryo X-ray microscopy analysis of both asexual and sexual stage intraerythrocytic parasites. Using the contrast mechanism provided by this modality the parasite and host cell surfaces are readily observed and the parasite nuclei can be distinguished from the cytoplasm. The iron-dense hemozoin is strongly X-ray absorbing and the rod-like nature of these structures is apparent. Neutral lipid bodies adjacent to the digestive vacuole are apparent in the trophozoite stage, and in the final stages of asexual development lipid-rich secretory organelles at the apical ends of daughter merozoites within the segmenting schizont are readily observed.

In the developing gametocyte, the parasite elongates by elaborating a sub-pellicular complex underneath the parasite membrane. This complex is not present in the trophozoite stage and comprises a double-membraned lamellar structure underpinned by a layer of microtubules (Sinden and Smalley, 1979). The extension of the sub-pellicular complex drives parasite elongation giving the gametocyte its characteristic falciform shape (Bannister et al., 2000). In the final stage of development, the ends become more rounded as the microtubule network is disassembled (Sinden et al., 1978).

Hemozoin crystals are readily observed in gametocytes showing that hemoglobin digestion takes place in the intraerythrocytic sexual stages as reported previously (Lang-Unnasch and Murphy, 1998; Sinden, 1982). In some late stage gametocytes the crystals are highly dispersed while in others they are more clumped. This is consistent with previous ultrastructural studies showing that in mature male gametocytes, hemozoin is contained

within multiple compartments, while mature female gametocytes have a central condensation of hemozoin crystals (Sinden, 1982).

The average volume of an uninfected RBC was found to be ~86 fL, in reasonable agreement with previous reports (88 fL (Lew et al., 1995); 93 fL (Park et al., 2008); 90–93 fL (Waugh et al., 1992)). We found that while the asexual parasite gradually increases in volume, the host RBC volume is concomitantly decreased so that the total volume is kept constant until early schizogony; it then decreases briefly before expanding again.

An important factor in volume control in asexual stage-infected RBCs is the appearance of the NPP in early trophozoite stages. The NPP provides both direct and indirect paths for the uptake of nutrients but leads to logistical problems with volume control (Martin and Kirk, 2007; Saliba et al., 2006). Early modeling suggested that the altered Na^+ and K^+ levels in the host cell cytoplasm would cause an increase in the volume of the infected RBC as the parasite matures (Staines et al., 2001). It was suggested this would substantively compromise the osmotic stability of the host cell in the last few hours before rupture (Staines et al., 2001).

This contrasts with measurements based on water content which indicate little change (Saliba et al., 1998) or even a decrease (Zanner et al., 1990) in the volume of the infected RBC during parasite development, and a recent analysis based on fluorescence confocal microscopy of calcein-loaded RBCs which suggested a moderate increase (1.17-fold) in volume in the trophozoite stage which is reversed in the schizont stage (Esposito et al., 2010). Our cryo X-ray microscopy analyses support the suggestion that the volume changes are moderate, with evidence for a small decrease in the volume of infected RBCs at the 8–16 nuclei stage.

The very moderate changes in infected RBC volume suggest that the increase in parasite volume is coupled to consumption of the host cell contents. Cryo X-ray microscopy permits an analysis of the concentration of carbon-based components in different compartments. This provides a direct means of measuring the amount and concentration of hemoglobin (assuming that hemoglobin is the main component present in the RBC cytoplasm) in RBCs infected with either asexual or sexual stage parasites. The hemoglobin tetramer concentration in uninfected RBCs was found to be ~5 mM, in good agreement with estimates from other methods (5.6 mM (Esposito et al., 2008), 4.8–5.4 mM (Hellerstein et al., 1970), 4.8 mM (Park et al., 2008)). Previous studies using a range of biophysical techniques have indicated a decrease in hemoglobin concentration in the infected RBC cytoplasm, as the asexual parasite develops to the schizont stage (Esposito et al., 2008; Mauritz et al., 2011; Park et al., 2008). Our cryo X-ray microscopy analysis for schizont-infected RBCs gives a value of ~2.7 mM, which is within the range reported using other methods, 3.7 mM (Esposito et al., 2008), 2.9 mM (Park et al., 2008), and 1.9–2.9 mmoles/10^{13} cells (Krugliak et al., 2002). Thus our data support the suggestion that the maintenance of RBC volume could be achieved by excess digestion of hemoglobin and efflux of the amino acids via the NPP (Lew et al., 2003).

Indeed our cryo-X-ray microscopy data permit a detailed analysis of the hemoglobin content at different stages. The concentration exhibits a biphasic pattern, remaining constant during the ring stage, then transitioning to a lower value as the parasite commences nuclear division. This corresponds to the point (~24 h after invasion) when the rate of hemoglobin digestion increases (Abu Bakar et al., 2010). The hemoglobin concentration is then sustained at a constant level during the period of the most intense hemoglobin digestion, i.e. the trophozoite and early schizont stages. The data indicate that the consumption of hemoglobin by the asexual parasite (which begins in the mid ring stage (Abu Bakar et al., 2010))

matches the expansion of the parasite up until the transition from the ring stage to the trophozoite stage. Thereafter hemoglobin digestion exceeds parasite growth while the infected RBC volume is maintained. As a result the hemoglobin concentration drops. In the final segmenter stage the hemoglobin concentration drops again perhaps due to a further increase in RBC permeability.

Changes in cellular organization during gametocyte development have not been studied extensively. The gametocyte undergoes a remarkable extension with a change in the length to width ratio from ~1:1 (stage II), ~2:1 (stage III), ~4:1 (stage IV) to ~3:1 Interestingly there is little change in the calculated mean volume of the maturing gametocyte despite the change in shape. It remains constant apart from a transient decrease in both parasite and total infected RBC volume at stage IV. At this point the parasite is fully extended, which deforms the host cell, and decreases the overall volume.

About 50% of the host hemoglobin is digested by the time the gametocyte is readily distinguished (stage II/III) and digestion appears to be completed by stage IV. This is consistent with reports that late stage gametocytes are much less sensitive to chloroquine and artemisinin (Peatey et al., 2009; Smalley, 1977). As for asexual stages hemoglobin digestion appears to exceed parasite growth. The concentration of hemoglobin is lower in stage III gametocytes compared with uninfected RBCs. It remains constant in stage IV, despite further digestion, due to a small decrease in the infected RBC volume. At stage V the dissipation of the microtubules network gives rise to a relaxation of the parasite and the RBC morphology leading to the recovery of the RBC volume and a decrease of the hemoglobin concentration. Volume control mechanisms have not been studied in the gametocyte stage but it appears likely that, as for the asexual stages, consumption of excess hemoglobin, and dispersal of the resultant amino acids, helps prevent osmotic swelling and stabilizes the circulating gametocyte.

5. Conclusion

We have shown that hemoglobin digestion and parasite growth are tightly coordinated in both asexual and sexual stage *P. falciparum* thus permitting an increase in parasite volume without causing premature host cell lysis. This work illustrates the usefulness of soft X-ray tomography as a tool for addressing important biological problems.

Supplementary Material

Refer to Web version on PubMed Central for supplementary material.

Acknowledgments

The authors acknowledge support from the Australian Academy of Science, the Australian Synchrotron, the Australian Research Council and the Australian National Health and Medical Research Council, the US Department of Energy, Office of Biological and Environmental Research (DE-AC02-05CH11231), the National Center for Research Resources of the National Institutes of Health (RR019664). Use of the Advanced Light Source was supported by the US Department of Energy, Office of Science. We thank Sam Deed and Rosanne Boudreau for technical support and Dr Richard Allen, Australian National University, for useful discussions.

Abbreviations

BSA	bovine serum albumin
NPP	novel permeability pathways
RBC	red blood cell

References

Abu Bakar NA, Klonis N, Hanssen E, Chan C, Tilley L. Digestive-vacuole genesis and endocytic processes in the early intraerythrocytic stages of *Plasmodium falciparum*. J. Cell Sci. 2010; 123:441–450. [PubMed: 20067995]

Alano P. *Plasmodium falciparum* gametocytes: still many secrets of a hidden life. Mol. Microbiol. 2007; 66:291–302. [PubMed: 17784927]

Alano P, Premawansa S, Bruce MC, Carter R. A stage specific gene expressed at the onset of gametocytogenesis in *Plasmodium falciparum*. Mol. Biochem. Parasitol. 1991; 46:81–88. [PubMed: 1852178]

Aley SB, Sherwood JA, Marsh K, Eidelman O, Howard RJ. Identification of isolate-specific proteins on sorbitol-enriched *Plasmodium falciparum* infected erythrocytes from Gambian patients. Parasitology. 1986; 92:511–525. [PubMed: 3526259]

Bannister LH, Hopkins JM, Fowler RE, Krishna S, Mitchell GH. A brief illustrated guide to the ultrastructure of *Plasmodium falciparum* asexual blood stages. Parasitol. Today. 2000; 16:427–433. [PubMed: 11006474]

Dixon MW, Thompson J, Gardiner DL, Trenholme KR. Sex in Plasmodium: a sign of commitment. Trends Parasitol. 2008; 24:168–175. [PubMed: 18342574]

Dixon MW, Peatey CL, Gardiner DL, Trenholme KR. A green fluorescent protein-based assay for determining gametocyte production in *Plasmodium falciparum*. Mol. Biochem. Parasitol. 2009; 163:123–126. [PubMed: 19027798]

Erdogan H, Fessler JA. Ordered subsets algorithms for transmission tomography. Phys. Med. Biol. 1999; 44:2835–2851. [PubMed: 10588288]

Esposito A, Tiffert T, Mauritz JM, Schlachter S, Bannister LH, et al. FRET imaging of hemoglobin concentration in *Plasmodium falciparum*-infected red cells. PLoS One. 2008; 3:e3780. [PubMed: 19023444]

Esposito A, Choimet JB, Skepper JN, Mauritz JM, Lew VL, et al. Quantitative imaging of human red blood cells infected with *Plasmodium falciparum*. Biophys. J. 2010; 99:953–960. [PubMed: 20682274]

Fivelman QL, McRobert L, Sharp S, Taylor CJ, Saeed M, et al. Improved synchronous production of *Plasmodium falciparum* gametocytes in vitro. Mol. Biochem. Parasitol. 2007; 154:119–123. [PubMed: 17521751]

Goldberg DE. Hemoglobin degradation. Curr. Top Microbiol. Immunol. 2005; 295:275–291. [PubMed: 16265895]

Gu W, Etkin LD, Le Gros MA, Larabell CA. X-ray tomography of *Schizosaccharomyces pombe*. Differentiation. 2007; 75:529–535. [PubMed: 17459084]

Hadley TJ, Erkmen Z, Kaufman BM, Futrovsky S, McGuinnis MH, et al. Factors influencing invasion of erythrocytes by *Plasmodium falciparum* parasites: the effects of an N-acetyl glucosamine neoglycoprotein and an anti-glycophorin A antibody. Am. J. Trop. Med. Hyg. 1986; 35:898–905. [PubMed: 3532846]

Hanssen E, Knoechel C, Klonis N, Abu-Bakar N, Deed S, et al. Cryo transmission X-ray imaging of the malaria parasite, *P. Falciparum*. J. Struct. Biol. 2011; 173:161–168. [PubMed: 20826218]

Hellerstein S, Spees W, Surapathana LO. Hemoglobin concentration and erythrocyte cation content. J. Lab. Clin. Med. 1970; 76:10–24. [PubMed: 5425358]

Jackson KE, Klonis N, Ferguson DJP, Adisa A, Dogovski C, et al. Food vacuole-associated lipid bodies and heterogeneous lipid environments in the malaria parasite, *Plasmodium falciparum*. Mol. Microbiol. 2004; 54:109–122. [PubMed: 15458409]

Jackson KE, Spielmann T, Hanssen E, Adisa A, Separovic F, et al. Selective permeabilization of the host cell membrane of *Plasmodium falciparum*-infected red blood cells with streptolysin O and equinatoxin II. Biochem. J. 2007; 403:167–175. [PubMed: 17155936]

Knight A, Sinden RE. The purification of gametocytes of *Plasmodium falciparum* and *P. Yoelii nigeriensis* by colloidal silica (Percoll) gradient centrifugation. Trans. R. Soc. Trop. Med. Hyg. 1982; 76:503–509. [PubMed: 6763789]

Kremer JR, Mastronarde DN, McIntosh JR. Computer visualization of three-dimensional image data using IMOD. J. Struct. Biol. 1996; 116:71–76. [PubMed: 8742726]

Krugliak M, Zhang J, Ginsburg H. Intraerythrocytic *Plasmodium falciparum* utilizes only a fraction of the amino acids derived from the digestion of host cell cytosol for the biosynthesis of its proteins. Mol. Biochem. Parasitol. 2002; 119:249–256. [PubMed: 11814576]

Lambros C, Vanderberg JP. Synchronization of *Plasmodium falciparum* erythrocytic stages in culture. J. Parasitol. 1979; 65:418–420. [PubMed: 383936]

Lang-Unnasch N, Murphy AD. Metabolic changes of the malaria parasite during the transition from the human to the mosquito host. Annu. Rev. Microbiol. 1998; 52:561–590. [PubMed: 9891808]

Larabell CA, Le Gros MA. X-ray tomography generates 3-D reconstructions of the yeast, *Saccharomyces cerevisiae*, at 60-nm resolution. Mol. Biol. Cell. 2004; 15:957–962. [PubMed: 14699066]

Le Gros MA, McDermott G, Larabell CA. X-ray tomography of whole cells. Curr. Opin. Struct. Biol. 2005; 15:593–600.

Lew VL, Tiffert T, Ginsburg H. Excess hemoglobin digestion and the osmotic stability of *Plasmodium falciparum*-infected red blood cells. Blood. 2003; 101:4189–4194. [PubMed: 12531811]

Lew VL, Raftos JE, Sorette M, Bookchin RM, Mohandas N. Generation of normal human red cell volume, hemoglobin content, and membrane area distributions by “birth” or regulation? Blood. 1995; 86:334–341. [PubMed: 7795242]

Lew VL, Macdonald L, Ginsburg H, Krugliak M, Tiffert T. Excess haemoglobin digestion by malaria parasites: a strategy to prevent premature host cell lysis. Blood Cells Mol. Dis. 2004; 32:353–359. [PubMed: 15121091]

Loria P, Miller S, Foley M, Tilley L. Inhibition of the peroxidative degradation of haem as the basis of action of chloroquine and other quinoline antimalarials. Biochem. J. 1999; 339:363–370. [PubMed: 10191268]

Martin RE, Kirk K. Transport of the essential nutrient isoleucine in human erythrocytes infected with the malaria parasite *Plasmodium falciparum*. Blood. 2007; 109:2217–2224. [PubMed: 17047158]

Mastronarde DN. Dual-axis tomography: an approach with alignment methods that preserve resolution. J. Struct. Biol. 1997; 120:343–352. [PubMed: 9441937]

Mauritz JM, Seear R, Esposito A, Kaminski CF, Skepper JN, et al. X-ray microanalysis investigation of the changes in Na, K, and hemoglobin concentration in *Plasmodium falciparum*-infected red blood cells. Biophys. J. 2011; 100:1438–1445. [PubMed: 21402025]

MedlinePlus, National Institutes of Health Website. http://www.nlm.nih.gov/medlineplus/ency/article/003648.htm.

Miller LH, Baruch DI, Marsh K, Doumbo OK. The pathogenic basis of malaria. Nature. 2002; 415:673–679. [PubMed: 11832955]

Nguitragool W, Bokhari AA, Pillai AD, Rayavara K, Sharma P, et al. Malaria parasite *clag3* genes determine channel-mediated nutrient uptake by infected red blood cells. Cell. 2011; 145:665–677. [PubMed: 21620134]

Pagola S, Stephens PW, Bohle DS, Kosar AD, Madsen SK. The structure of malaria pigment β-haematin. Nature. 2000; 404:307–310. [PubMed: 10749217]

Park Y, Diez-Silva M, Popescu G, Lykotrafitis G, Choi W, et al. Refractive index maps and membrane dynamics of human red blood cells parasitized by *Plasmodium falciparum*. Proc. Natl. Acad. Sci. U S A. 2008; 105:13730–13735. [PubMed: 18772382]

Parkinson DY, McDermott G, Etkin LD, Le Gros MA, Larabell CA. Quantitative 3-D imaging of eukaryotic cells using soft X-ray tomography. J. Struct. Biol. 2008; 162:380–386. [PubMed: 18387313]

Peatey CL, Skinner-Adams TS, Dixon MW, McCarthy JS, Gardiner DL, et al. Effect of antimalarial drugs on *Plasmodium falciparum* gametocytes. J. Infect. Dis. 2009; 200:1518–1521. [PubMed: 19848586]

Ponnudurai T, Lensen AHW, Meis J, Meuwissen J. Synchronization of *Plasmodium falciparum* gametocytes using an automated suspension culture system. Parasitology. 1986; 93:263–274. [PubMed: 3537921]

Rabiner SF, Helbert JR, Lopas H, Friedman LH. Evaluation of a stroma-free hemoglobin solution for use as a plasma expander. J. Exp. Med. 1967; 126:1127–1142. [PubMed: 6058496]

Rowe JA, Claessens A, Corrigan RA, Arman M. Adhesion of *Plasmodium falciparum*-infected erythrocytes to human cells: molecular mechanisms and therapeutic implications. Expert. Rev. Mol. Med. 2009; 11:e16. [PubMed: 19467172]

Saliba KJ, Horner HA, Kirk K. Transport and metabolism of the essential vitamin pantothenic acid in human erythrocytes infected with the malaria parasite *Plasmodium falciparum*. J. Biol. Chem. 1998; 273:10190–10195. [PubMed: 9553068]

Saliba KJ, Martin RE, Broer A, Henry RI, McCarthy CS, et al. Sodium-dependent uptake of inorganic phosphate by the intracellular malaria parasite. Nature. 2006; 443:582–585. [PubMed: 17006451]

Sinden RE. Gametocytogenesis of *Plasmodium falciparum* in vitro: an electron microscopic study. Parasitology. 1982; 84:1–11. [PubMed: 7038594]

Sinden RE, Smalley ME. Gametocytogenesis of *Plasmodium falciparum* in vitro - Cell cycle. Parasitology. 1979; 79:277–296. [PubMed: 395486]

Sinden RE, Canning EU, Bray RS, Smalley ME. Gametocyte and gamete development in *Plasmodium falciparum*. Proc. R. Soc. Lond. B Biol. Sci. 1978; 201:375–399. [PubMed: 27809]

Smalley ME. *Plasmodium falciparum* gametocytes: The effect of chloroquine on their development. Trans. R. Soc. Trop. Med. Hyg. 1977; 71:526–529. [PubMed: 343314]

Snell SM, Marini MA. A convenient spectroscopic method for the estimation of hemoglobin concentrations in cell-free solutions. J. Biochem. Biophys. Methods. 1988; 17:25–33. [PubMed: 3235763]

Staines HM, Ellory JC, Kirk K. Perturbation of the pump-leak balance for Na(+) and K(+) in malaria-infected erythrocytes. Am. J. Physiol. Cell Physiol. 2001; 280:C1576–C1587. [PubMed: 11350753]

Stayman JW, Fessler JA. Regularization for uniform spatial resolution properties in penalized-likelihood image reconstruction. IEEE Trans. Med. Imaging. 2000; 19:601–615. [PubMed: 11026463]

Tilley L, Dixon MW, Kirk K. The *Plasmodium falciparum*-infected red blood cell. Int. J. Biochem. Cell Biol. 2011; 43:839–842. [PubMed: 21458590]

Trang DT, Huy NT, Kariu T, Tajima K, Kamei K. One-step concentration of malarial parasite-infected red blood cells and removal of contaminating white blood cells. Malar J. 2004; 3:7. [PubMed: 15025790]

Uchida M, McDermott G, Wetzler M, Le Gros MA, Myllys M, et al. Soft X-ray tomography of phenotypic switching and the cellular response to antifungal peptoids in *Candida albicans*. Proc. Natl. Acad. Sci. U S A. 2009; 106:19375–19380. [PubMed: 19880740]

Waugh RE, Narla M, Jackson CW, Mueller TJ, Suzuki T, et al. Rheologic properties of senescent erythrocytes: loss of surface area and volume with red blood cell age. Blood. 1992; 79:1351–1358. [PubMed: 1536958]

WHO. World Malaria Report 2010. 2010. http://www.who.int/malaria/world_malaria_report_2010/world_malaria_report_2010.pdf

Zanner MA, Galey WR, Scaletti JV, Brahm J, Jagt DL. Water and urea transport in human erythrocytes infected with the malaria parasite *Plasmodium falciparum*. Mol. Biochem. Parasitol. 1990; 40:269–278. [PubMed: 2194124]

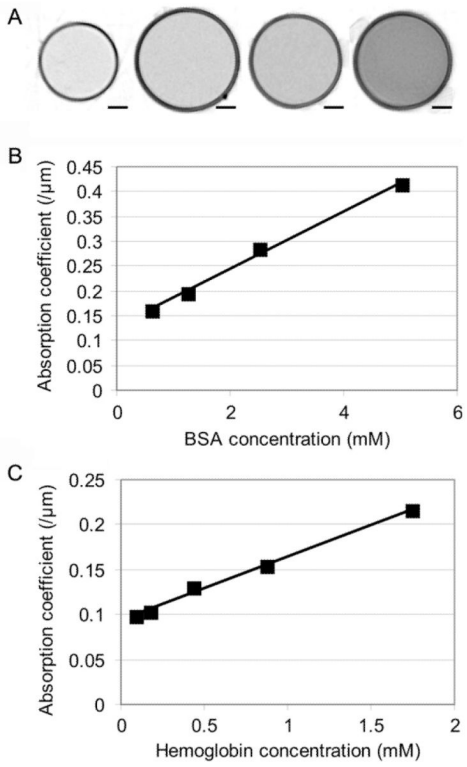

Fig.1.

Estimation of the absorption coefficients of BSA and hemoglobin. (A) Virtual z-sections through transmission X-ray tomograms of capillaries containing BSA at concentration ranging from 5 to 0.625 mM. The circular profiles represent the walls of the glass capillaries viewed in cross-section. (B and C) Absorption coefficients plotted against BSA (B) and hemoglobin (C) concentrations. The absorption curve does not go through zero due to some absorption of soft X-rays by water or PBS. Scale bars: 1 μm.

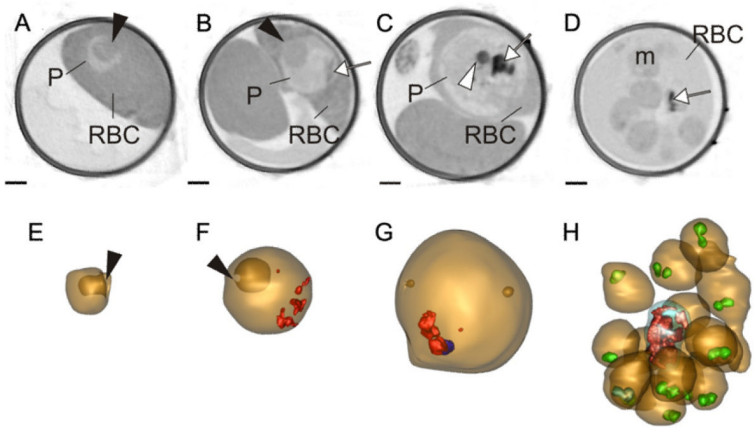

Fig.2.

Transmission X-ray tomography of asexual stages of *P. falciparum*. (A–D) Individual virtual z-sections (66 nm) of RBCs infected with ring, early and late trophozoites and a segmented schizont. The parasites (P) are indicated. (E-H) Rendered models generated by segmentation of the tomograms. In the models the parasite surface is depicted in gold and the hemozoin crystals in red. Invaginations of the parasite surface are depicted in deeper gold. In the segmenting schizont the rhoptry pairs in each of the nascent daughter cells are rendered in green and the digestive vacuole in blue. The ring stage parasite (A and E) is invaginated (black arrowheads) to form a cup shape. The invagination persists, with a smaller opening, (black arrowheads) in the early trophozoite (B and F), and the first evidence of hemozoin (white arrow) is visible (B and F). An early schizont (C and G) has 8 nuclei, an accumulation of hemozoin (white arrow) and an X-ray dense lipid body (white arrowhead). A segmented schizont (D and H) has 16 daughter cells, and shows a decrease in hemoglobin density. Hemozoin (D, white arrow; H, red crystals) accumulates in the digestive vacuole in a central remnant body. Scale bars: 1 μm.

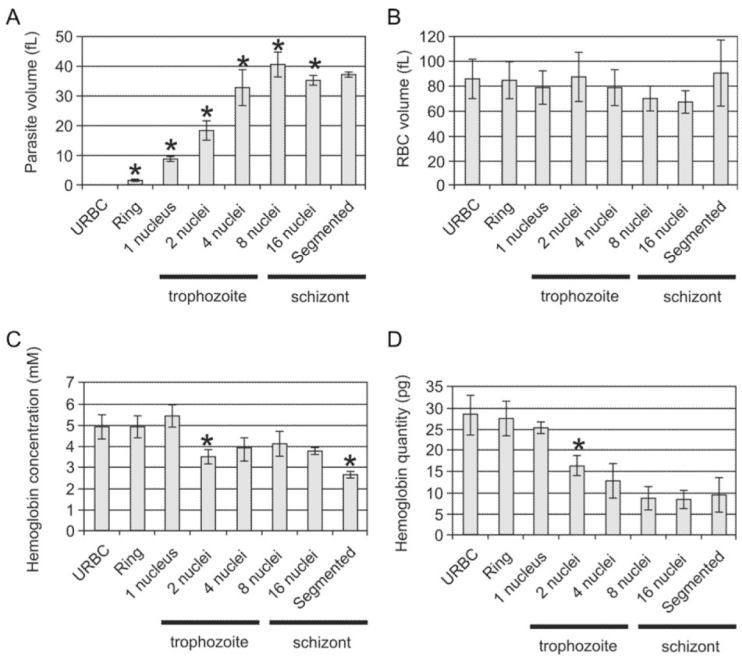

Fig.3.

Analysis of morphometric parameters for asexual stage parasites at different stages of development. The tomograms were segmented manually and the models used to estimate the volumes of the parasites (A) and the infected RBCs (B). The absorption coefficient (see Fig. 1) was applied to determine the hemoglobin concentration in the RBC cytoplasm (C). The total amount of hemoglobin (D) was calculated from the known volume and concentration. The asterisks indicate measurement that are significantly different ($P < 0.05$) from the value for the previous stage.

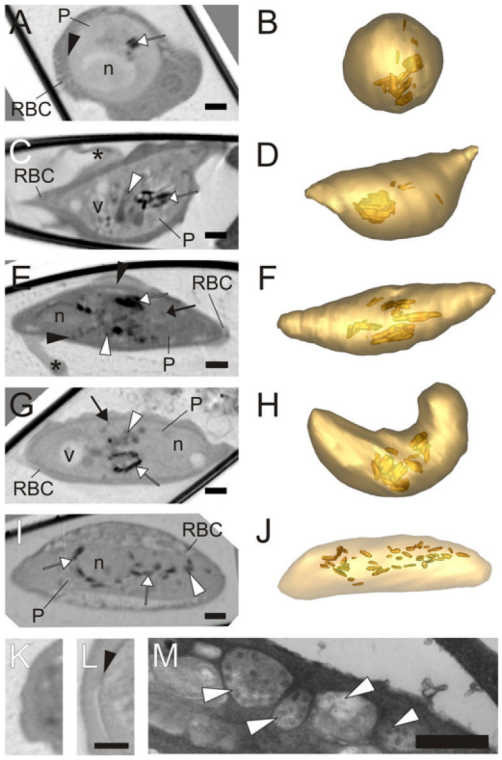

Fig.4.

Transmission X-ray tomography of sexual stages of *P. falciparum*. (A–J; Left panels) Individual virtual sections (64 nm) of gametocytes at stages II–V. (Right panels) Rendered models generated by segmentation of the tomograms. The parasite surface is depicted in light gold and the hemozoin crystals in deeper gold. In the tomograms the mitochondrion is indicated with a white arrow, the sub-pellicular complex with a black arrowhead, hemozoin crystals with a white arrow and dense granules (likely to be osmophillic bodies) with a black arrow. The nucleus (n), vacuoles (v) and Laveran's bib (*) are marked. The stage II gametocyte (A and B) is roughly spherical and exhibits evidence of a sub-pellicular membrane complex (see Panel L). By stage III (C and D) formation of the crescent shape is initiated with elongation along one side. The stage IV gametocyte (E and F) is elongated with protruding extremities and shows a distinctive sub-pellicular membrane complex (black arrowhead). Some osmophillic bodies start to appear and the Laveran's bid is evident. Stage V gametocytes (G–J) have more rounded ends and a less obvious sub-pellicular membrane complex, and prominent osmophillic bodies and mitochondrion. See Supp. Movie 1 for a translation through the tomogram shown in G. (I and J) Distribution of the hemozoin crystals in a fixed male gametocyte. (I) Virtual slice through the reconstructed tomogram of a fixed male gametocyte. (J) Segmentation model with the surface of the parasite in pale gold and the hemozoin crystals in deeper gold. (K and L) Virtual sections showing the transition between the parasite cytoplasm and the RBC cytoplasm for an asexual stage trophozoite (K) and a stage II gametocyte (L). The X-ray density at the parasite surface (arrowhead) probably represents the microtubule supported sub-pellicular membrane complex. (M) Section through a gametocyte prepared for electron microscopy. The arrowheads point to sections through the extended multi-globular mitochondrion that is present in the gametocyte. Scale bars (A–L): 1 μm; (M): 500 nm.

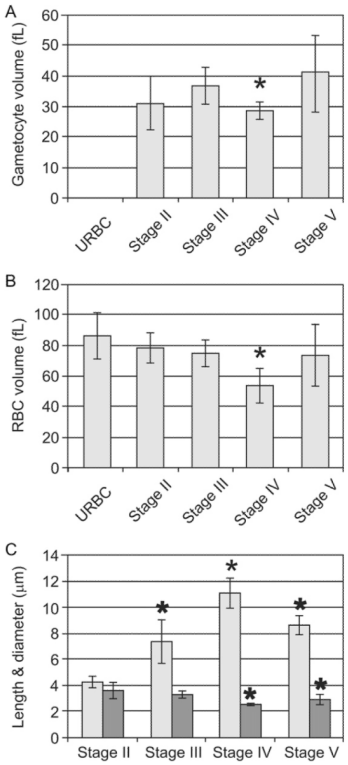

Fig.5.

Morphometric parameters at different stages of gametocyte development. The tomograms were segmented manually and used to estimate the volumes of (A) the parasite and (B) the infected RBC, as well as (C) the average length (pale grey) and diameter (dark grey) of each parasite stage.

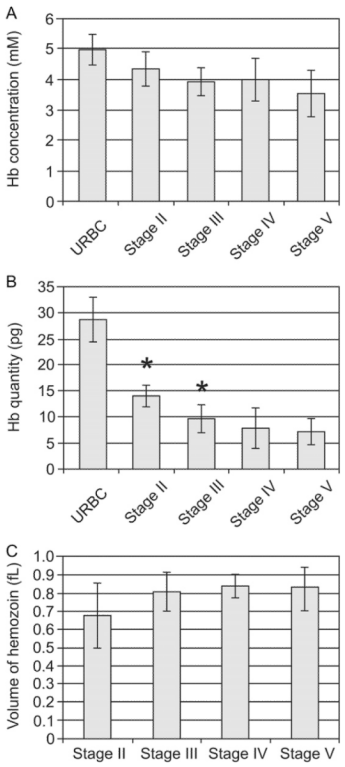

Fig. 6.

Analysis of hemoglobin concentration and hemozoin volume at different stages of gametocyte development. The absorption coefficient (see Fig. 1) was applied to determine the hemoglobin concentration in the RBC cytoplasm (A). The total amount of hemoglobin (B) was calculated from the volume and concentration. (C) The volumes of the hemozoin crystals during gametogenesis were estimated by analysis of rendered models using IMODinfo. The asterisks indicate measurements that are significantly different ($P < 0.05$) from the value for the previous stage.